

Pulse shaping and coherent Raman spectroscopy in condensed phases

Y. J. Yan and S. Mukamel

Department of Chemistry, University of Rochester, Rochester, New York 14627

(Received 5 June 1990; accepted 10 October 1990)

A microscopic theory for ultrafast coherent Raman spectroscopy of polyatomic molecules in condensed phases is developed. For off resonant excitation, an effective Hamiltonian that controls the molecular dynamics in a Raman process is derived. The limitations of the driven oscillator model are clarified, and generalized equations of motion, which hold for resonant and off resonant excitation, are derived. Spectral selectivity using pulse shaping is discussed.

I. INTRODUCTION

Coherent Raman scattering using femtosecond laser pulses is widely used as a probe for elementary molecular nuclear motions in condensed phases.¹⁻⁴ In an impulsive stimulated light scattering (ISLS) experiment, a single laser pulse is applied and coherent molecular motions whose time scales are slower than the pulse are observed in the time domain. In this technique, all Raman active modes are excited. The development of femtosecond pulse shaping techniques⁵ has made it possible to optically control these elementary molecular motions. In a recent experiment, a terahertz train of femtosecond pulses was used to excite an α -perylene crystal.⁶ Only the optical phonon whose frequency equals to the inverse of the train interval is effectively excited, contributing to the macroscopic polarization of the medium, whereas the motions along other degrees of freedom with different frequencies are discriminated against.

A classical theory of off-resonant stimulated impulsive light scattering based on the molecular dielectric response, with linear coupling to the optically active modes in the ground electronic state was developed by Nelson and co-workers.^{1,2} This theory provides a clear and simple picture of the process. The quantum impulsive light scattering theories in the weak field limit developed recently by Chesnoy and Mokhtari,^{3a} Walsley, Wise, and Tang,^{3b} Walsh and Loring^{3c} are based on solving the Bloch equations perturbatively with respect to the external field. In these theories the molecular system is modeled as two manifolds of vibronic levels associated with the electronic excited and ground states, respectively. These theories are valid for both resonant and the off-resonant excitation processes. We have recently developed a doorway/window density matrix formalism for time-resolved optical spectroscopy in the weak field limit.⁷ The doorway/window formalism provides a clear physical picture of time-resolved optical processes. In this paper, we apply the doorway/window picture to develop a microscopic quantum mechanical theory for off-resonant light scattering with an arbitrary excitation intensity. The theory is valid for anharmonic vibrational motions with an arbitrary dependence of the electronic polarizability on nuclear coordinates, and the classical limit of the theory can be readily obtained. Extension to near-resonance excitation is discussed as well. In Sec. II, we use the density matrix and doorway/window picture to derive a general expression for

coherent off resonant Raman scattering. The optical signal [cf. Eq. (10)] is expressed in terms of the expectation value of the molecular polarizability calculated using the time-dependent doorway state prepared by the pump field. The molecular dynamics are controlled by an effective Hamiltonian [cf. Eq. (5)], which consists of the nuclear adiabatic Hamiltonian associated with the ground electronic state, and a time-dependent driving force which is proportional to the square of the pump Rabi frequency, scaled by its detuning from the electronic transition. The effective Hamiltonian holds for an arbitrary time dependence of the excitation field and an arbitrary coordinate dependence of the electronic transition dipole. In Sec. III, we consider the weak pump field limit in which the optical signal can be expressed in terms of the equilibrium response function of the molecular electronic polarizability. We further consider the lowest non-Condon effect in which the polarizability depends linearly on nuclear coordinates. In this case we recover the linearly driven Brownian harmonic oscillator model which has been widely used in the theory of impulsive Raman scattering.^{1,2} In Sec. IV, we discuss the consequences of pulse shaping and present a model calculation to demonstrate its frequency filtering effect, in which only the Raman active mode with a selected frequency is effectively excited. Finally, in Sec. V we interpret the pulse shaping experiment by examining the molecular density matrix, and discuss its implication on laser selective chemistry.

II. OFF RESONANT COHERENT RAMAN SCATTERING

Consider an optically thin medium interacting with an external laser field. The total Hamiltonian in the electric dipole approximation is

$$H_T(\mathbf{r}, t) = H - V\mathbf{E}(\mathbf{r}, t), \quad (1a)$$

$$H = |g\rangle H_g \langle g| + |e\rangle (H_e + \omega_{eg}) \langle e|, \quad (1b)$$

$$V = \mu(\mathbf{q}) [|g\rangle \langle e| + |e\rangle \langle g|]. \quad (1c)$$

The system consists of a solution of chromophores with two electronic states $|g\rangle$ and $|e\rangle$ and the corresponding nuclear adiabatic Hamiltonians H_g and H_e . Here, ω_{eg} denotes the 0-0 electronic transition frequency and V represents the electronic transition dipole. The present theory holds also for the optical phonons studied by Nelson *et al.*⁶ provided the phonon bandwidth is narrower than the inverse timescale of

the experiment. In this case spatial dispersion can be neglected and an Einstein model for the optical phonon can be used. Coherent Raman scattering is often carried out in a transient grating configuration,^{1,2,6} in which the system is first subject to two identical pulses with the mean frequency Ω_p and wave vectors \mathbf{k}_1 and \mathbf{k}_2 , which create a dynamical grating with wave vector $\mathbf{k}_1 - \mathbf{k}_2$. Following a delay time τ_D , the system is probed using a third pulse with mean frequency Ω_T and wave vector \mathbf{k}_3 . The coherent Raman scattering signal is detected at the direction $\mathbf{k}_S = \mathbf{k}_3 + \mathbf{k}_1 - \mathbf{k}_2$ corresponding to the Bragg diffraction off the grating, and is recorded as the function of the delay time τ_D . The external field in Eq. (1a) is

$$E(\mathbf{r}, t) = E_p(\mathbf{r}, t) + E_T(\mathbf{r}, t), \quad (2a)$$

$$E_p(\mathbf{r}, t) = E_p(t) \exp(-i\Omega_p t) [\exp(i\mathbf{k}_1 \mathbf{r}) + \exp(i\mathbf{k}_2 \mathbf{r})] + \text{c.c.}, \quad (2b)$$

$$E_T(\mathbf{r}, t) = E_T(t - \tau_D) \exp(i\mathbf{k}_3 \mathbf{r} - i\Omega_T t) + \text{c.c.} \quad (2c)$$

Here, c.c. denotes the complex conjugate; $E_p(t)$ and $E_T(t - \tau_D)$ denote the temporal envelopes of the pump and the delayed probe fields, respectively.

We shall calculate the transient Raman scattering line shape when the pump and the probe are well separated. We can then use the doorway/window picture of pump-probe spectroscopy,⁷ where the pump field prepares the doorway state, which is then detected through the window defined by the probe field.

Let us start with the preparation process and define the doorway state. For a molecule located at position \mathbf{r} , the molecular density matrix is represented in the form:

$$\rho_T(\mathbf{r}, t) = |g\rangle \rho_{gg}(\mathbf{r}, t) \langle g| + |e\rangle \rho_{ee}(\mathbf{r}, t) \langle e| + |e\rangle \rho_{eg}(\mathbf{r}, t) \langle g| + |g\rangle \rho_{ge}(\mathbf{r}, t) \langle e|, \quad (3)$$

where each matrix element ρ_{mn} , with $m, n = e, \text{ or } g$, is an operator in the molecular nuclear space; ρ_{gg} or ρ_{ee} describes the nuclear dynamics when the medium is in the electronic ground or excited state, whereas ρ_{eg} or ρ_{ge} represents the nuclear dynamics when the system is in an electronic (optical) coherence. The four coupled Heisenberg equations of motion of $\rho_{mn}(\mathbf{r}, t)$ are given in Appendix A [Eq. (A2)]. In this paper, we shall focus on off resonant Raman spectroscopy, in which the pump and the probe electronic detunings $\omega_{eg} \pm \Omega_p$ and $\omega_{eg} \pm \Omega_T$ are large compared with the inverse time scales of the excitation pulses and the molecular nuclear dynamics. In this case the equations of motion for ρ_{gg} and ρ_{ee} are decoupled. Since the system is initially in the ground electronic state, the state prepared by the pump (the doorway state) is characterized only by $\rho_{gg}(\mathbf{r}, t)$, which satisfies the equation of motion (cf. Appendix A):

$$\dot{\rho}_{gg}(\mathbf{r}, t) = -(i/\hbar) [H_{\text{eff}}(\mathbf{r}, t), \rho_{gg}(\mathbf{r}, t)]. \quad (4)$$

Here the effective Hamiltonian is⁸

$$H_{\text{eff}}(\mathbf{r}, t) \equiv H_g - 2[1 + \cos(\mathbf{k}_1 - \mathbf{k}_2) \mathbf{r}] \alpha_p |E_p(t)|^2 \quad (5a)$$

and

$$\alpha_p \equiv \frac{\mu^2}{\hbar} \left[\frac{1}{\omega_{eg} - \Omega_p} + \frac{1}{\omega_{eg} + \Omega_p} \right] \quad (5b)$$

is the electronic polarizability at frequency Ω_p . Equations (4)–(5) are valid for an arbitrary intensity and shape of the pump field. It should be noted that the present theory is not limited to the transient grating configuration. It generally holds for any doorway state prepared by an off resonant excitation process which could involve for example only a single excitation pulse.^{1,2} For resonant excitation, the molecular dynamics depend also on the electronic excited state Hamiltonian H_e .^{3,7} In this case, the equations of motion for ρ_{gg} and ρ_{ee} are coupled (cf. Appendix A) and the effective Hamiltonian formalism is inapplicable.

We shall be interested in the $\mathbf{k}_1 - \mathbf{k}_2$ spatial Fourier component of the doorway state that constitutes the relevant Raman grating:

$$\rho(t) \equiv \int d\mathbf{r} \exp[-i(\mathbf{k}_1 - \mathbf{k}_2) \mathbf{r}] \rho_{gg}(\mathbf{r}, t). \quad (6)$$

We shall now consider the detection process using a weak probe field delayed by τ_D with respect to the pump field, and calculate the coherent Raman scattering signal from the prepared doorway state. The coherent Raman signal in the direction $\mathbf{k}_S = \mathbf{k}_3 + \mathbf{k}_1 - \mathbf{k}_2$ is given by^{9,10}

$$S(\tau_D) = \int_{-\infty}^{\infty} dt |P(\mathbf{k}_S, t)|^2, \quad (7)$$

with

$$P(\mathbf{k}_S, t) = \int d\mathbf{r} \exp(-i\mathbf{k}_S \mathbf{r} + i\Omega_T t) P(\mathbf{r}, t). \quad (8)$$

This polarization can further be expressed in terms of the nonequilibrium molecular dipole-dipole correlation function (cf. Appendix B) calculated using the doorway state $\rho(t)$ [Eq. (6)]. The evaluation of the dipole-dipole correlation function generally involves complicated molecular nuclear dynamics.¹¹ In the case of off resonant probe detection, the nuclear dynamics in the dipole-dipole correlation can be neglected^{12,13} and we obtain (cf. Appendix B)

$$P(\mathbf{k}_S, t) = E_T(t - \tau_D) \text{Tr}[\alpha_T \rho(t)]. \quad (9)$$

Here, α_T is the molecular polarizability at the probe frequency, given by Eq. (5b) with replacing Ω_p by Ω_T . Substituting Eq. (9) for Eq. (7), we get

$$S(\tau_D) = \int_{-\infty}^{\infty} dt |E_T(t - \tau_D)|^2 \{\text{Tr}[\alpha_T \rho(t)]\}^2. \quad (10)$$

Equation (10) together with (4) and (5) constitute the formal basis of this paper. They are valid for arbitrary (anharmonic) nuclear adiabatic Hamiltonians H_g or H_e , arbitrary shapes of the pulse envelopes $E_p(t)$ and $E_T(t)$ and any intensity of the pump field. The probe field is assumed to be weak. The key quantity in the calculation of the spectral signal [Eq. (10)] is $\text{Tr}[\alpha_T \rho(t)]$, the expectation value of the molecular electronic polarizability with respect to the time-dependent doorway state [Eq. (4)]. The electronic polarizability (α_p or α_T) depends parametrically on the nuclear coordinates. The Raman active modes are characterized by a relatively strong coordinate dependence and the Raman signal reflects their coherent motions.^{13,14} Nuclear motions that do not affect the polarizability do not show up in the spectrum. In the following section we shall consider

some limiting cases, in which the calculation is further simplified.

III. COHERENT RAMAN USING WEAK FIELDS; THE NUCLEAR RESPONSE FUNCTION

When the pump and the probe fields are weak, we can expand the dynamics of ρ_{gg} [Eqs. (4) and (5)] to lowest order in $|E_p(t)|^2$. We then have¹³

$$\text{Tr}[\alpha_T \rho(t)] = \int_0^\infty d\tau |E_p(t-\tau)|^2 \langle (i/\hbar) [\alpha_T(\tau), \alpha_P(0)] \rangle. \quad (11)$$

The molecular nuclear dynamics is, in this case, described by the *response function*¹⁵ of the polarizability:

$$\langle (i/\hbar) [\alpha_T(\tau), \alpha_P(0)] \rangle \equiv (i/\hbar) \text{Tr} \{ [\alpha_T(\tau) \alpha_P(0) - \alpha_P(0) \alpha_T(\tau)] \rho_{eq} \}. \quad (12)$$

Here, ρ_{eq} is the equilibrium nuclear density matrix of the system in the ground electronic state and

$$\alpha_j(\tau) \equiv \exp(iH_g \tau / \hbar) \alpha_j \exp(-iH_g \tau / \hbar); \quad j = P, T. \quad (13)$$

Using Eq. (11), the coherent Raman signal [Eq. (10)] reduces to

$$S(\tau_D) = \int_{-\infty}^{\infty} dt |E_T(t - \tau_D)|^2 \times \left[\int_0^\infty d\tau |E_p(t - \tau)|^2 \langle (i/\hbar) [\alpha_T(\tau), \alpha_P(0)] \rangle \right]^2. \quad (14)$$

The effect of the pump field spectrum on Raman signal can be easily seen when the pump and probe are well separated. In this case we may change the lower integration limit of τ to $-\infty$ and Eq. (14) reduces to

$$S(\tau_D) \approx \int_{-\infty}^{\infty} dt |E_T(t - \tau_D)|^2 \times \left| \frac{1}{2\pi} \int_{-\infty}^{\infty} d\omega \exp(-i\omega t) I_P(\omega) R(\omega) \right|^2, \quad (15)$$

where

$$I_P(\omega) \equiv \int_{-\infty}^{\infty} dt \exp(i\omega t) |E_p(t)|^2, \quad (16a)$$

$$R(\omega) \equiv \int_{-\infty}^{\infty} dt \exp(i\omega t) \langle (i/\hbar) [\alpha_T(\tau), \alpha_P(0)] \rangle. \quad (16b)$$

As shown in Eq. (15), the spectral profile of the pump field $I_P(\omega)$ provides a *frequency filtering* function for the Raman signal. In the impulsive pump limit, $I_P(\omega)$ is independent of frequency and all the Raman modes contribute equally to the signal [Eq. (15)]. If a train of femtosecond pulses is used, $I_P(\omega)$ becomes a sharply localized function around some selected frequencies $\omega = n\omega_0$; $n = 1, 2, \dots$ In this case the pump excitation creates a frequency grating pattern within the optical medium and filters out a few Raman modes with frequencies around $n\omega_0$, while discriminating against other nuclear motions. This filtering effect will be illustrated further in the following sections.

Off resonant Raman scattering is induced by the dependence of the electronic polarizability on the nuclear coordinates $\alpha = \alpha(\mathbf{q})$. Usually this dependence is weak and in the Condon approximation, which is often used for resonant excitation, it may be neglected.^{9,14} Making use of this weak dependence, we expand $\alpha(\mathbf{q})$ to first order around the equilibrium configuration \mathbf{q}^0 :

$$\alpha_P(\mathbf{q}) = \alpha_P(\mathbf{q}^0) + \sum_j \kappa_j q_j + \dots, \quad (17a)$$

$$\alpha_T(\mathbf{q}) = \alpha_T(\mathbf{q}^0) + \sum_j \kappa'_j q_j + \dots. \quad (17b)$$

Here, $\kappa_j \equiv \partial \alpha_P / \partial q_j$ evaluated at \mathbf{q}^0 and κ'_j is defined similarly. In this case we have [cf. Eq. (5a)]

$$H_{\text{eff}}(\mathbf{r}, t) = H_g - 2[1 + \cos(\mathbf{k}_1 - \mathbf{k}_2) \cdot \mathbf{r}] \sum_j F_j(t) q_j, \quad (18a)$$

where

$$F_j(t) \equiv \kappa_j |E_p(t)|^2. \quad (18b)$$

is the *driving force* for the j th mode. If the q_j vibrations are harmonic we obtain the *driven oscillator* model.^{1,2} We have neglected the pure Condon term since it does not contribute to the doorway state $\rho(t)$ or $\rho_{gg}(\mathbf{r}, t)$ [Eq. (4)]. The signal [Eq. (14)] becomes

$$S(\tau_D) = \int_{-\infty}^{\infty} dt |E_T(t - \tau_D)|^2 \times \left[\int_0^\infty d\tau |E_p(t - \tau)|^2 \times \sum_{j,k} \kappa'_j \kappa_k \langle (i/\hbar) [q_j(\tau), q_k(0)] \rangle \right]^2, \quad (19a)$$

with

$$q_j(t) \equiv \exp(iH_g t / \hbar) q_j \exp(-iH_g t / \hbar). \quad (19b)$$

When the nuclear motions are classical we can use the classical response function.¹⁵ For Eq. (12) we have

$$\langle (i/\hbar) [\alpha_T(\tau), \alpha_P(0)] \rangle \approx \sum_j \frac{1}{M_j k_B T_B} \left\langle \alpha_T(\tau) \frac{\partial \alpha_P}{\partial q_j} p_j \right\rangle, \quad (20a)$$

and in Eq. (19a) we substitute

$$\langle (i/\hbar) [q_j(\tau), q_k(0)] \rangle \approx \frac{1}{M_k k_B T_B} \langle q_j(\tau) p_k \rangle, \quad (20b)$$

where M_j is the mass and p_j is the momentum of model j ; k_B is the Boltzmann constant and T_B is the temperature.

IV. THE DRIVEN BROWNIAN OSCILLATOR AND PULSE SHAPING

The nuclear dynamics of a polyatomic molecule in solution can often be described using the Brownian oscillator model, in which the ground state Hamiltonian H_g in Eq. (19b) represents harmonic Brownian motions; that is, the j th mode satisfies the generalized Langevin equations:^{11,16}

$$\dot{q}_j(t) = p_j(t)/M_j, \quad (21a)$$

$$\dot{p}_j(t) = -M_j\omega_j^2 q_j(t) - \int_{-\infty}^t d\tau \hat{\gamma}_j(t-\tau)p_j(\tau) + f_j(t). \quad (21b)$$

Here, $\hat{\gamma}_j(t)$ and $f_j(t)$ denote, respectively, the non-Markovian friction kernel and Gaussian stochastic random force acting on the j th mode with frequency ω_j . They satisfy the fluctuation-dissipation relation:^{11,16} $\langle f_j(t)f_k(0) \rangle = M_j \hat{\xi}_j \hat{\gamma}_j(t) \delta_{jk}$. Here, δ_{jk} is the Kronecker delta,

$$\xi_j = \hbar\omega_j(\bar{n}_j + 1/2) \quad (22a)$$

and

$$\bar{n} = [\exp(\hbar\omega_j/k_B T_B) - 1]^{-1} \quad (22b)$$

are the thermally averaged energy and occupation number of the j th oscillator at temperature T_B , respectively. The response function of the Brownian harmonic oscillator [Eq. (21)] is^{11,16}

$$\begin{aligned} \langle (i/\hbar)[q_j(t), q_k] \rangle &= \frac{1}{2} \frac{\langle q_j(\tau)p_j \rangle + \langle p_j q_j(\tau) \rangle}{\langle p_j^2 \rangle - \langle p_j \rangle^2} \delta_{jk} \\ &= (M_j\omega_j)^{-1} L^{-1} \left\{ \frac{\omega_j}{s^2 + s\gamma_j(s) + \omega_j^2} \right\} \delta_{jk} \end{aligned}$$

$$Z_j(t) = \begin{cases} (\omega_j/\bar{\omega}_j) \exp(-\gamma_j t/2) \sin \bar{\omega}_j t, & \gamma_j < 2\omega_j, \\ (\gamma_j t/2) \exp(-\gamma_j t/2), & \gamma_j = 2\omega_j, \\ [(\gamma_j/\omega_j)^2 - 4]^{-1/2} [\exp(-s_- t) - \exp(-s_+ t)], & \gamma_j > 2\omega_j, \end{cases} \quad (25a)$$

with

$$\bar{\omega}_j = (\omega_j^2 - \gamma_j^2/4)^{1/2}, \quad (25b)$$

$$s_{\pm} = \gamma_j/2 \pm (\gamma_j^2/4 - \omega_j^2)^{1/2}, \quad (25c)$$

where the three cases represent an underdamped, critically damped, and overdamped motion, respectively.

In concluding this section, we present model calculations that demonstrate the filtering effect of pulse shaping on a model molecule with three Raman active modes. For simplicity we assume that the probe scattering is impulsive, whereas the pump field consists of a train of N identical ultrashort pulses with

$$|E_p(t)|^2 = \frac{I_p(0)}{N} \sum_{n=1}^N \delta[t + (n-1)T]. \quad (26)$$

Here, T denotes the train period and the pulse train energy $I_p(0)$ [Eq. (16a)] remains unchanged when the total number of pulses N is varied. In this case the power spectrum of pump field intensity [Eq. (16a)] is given by

$$I_p(\omega) = I_p(0) \exp[-i(N-1)\omega T/2] \frac{\sin(N\omega T/2)}{N \sin(\omega T/2)}. \quad (27)$$

In the ordinary impulsive pump limit (the ISLS experiment), we have $N=1$ and $I_p(\omega) = I_p(0)$. As shown in Fig. 1, when the number of pulses in the pump train N increases, the spectral profile of pump field $|I_p(\omega)|^2$ is narrowed. Its maximum $I_p(0)$ remains, however, the same. Figure 1 dem-

$$\equiv \frac{1}{M_j\omega_j} Z_j(t-\tau)\delta_{jk}. \quad (23)$$

Here, L^{-1} denotes the inverse Laplace transform and $\gamma_j(s)$ is the Laplace transform of $\hat{\gamma}_j(t)$. The coherent Raman scattering signal [Eq. (19a)] in this case reduces to

$$\begin{aligned} S(\tau_D) &= \int_{-\infty}^{\infty} dt |E_T(t-\tau_D)|^2 \\ &\times \left[\int_0^{\infty} d\tau |E_p(t-\tau)|^2 \sum_j \frac{\kappa_j \kappa'_j}{M_j\omega_j} Z_j(\tau) \right]^2. \end{aligned} \quad (24)$$

In the *impulsive excitation configuration*, where the durations of the pump and probe pulses are short compared with the molecular nuclear dynamics, we may approximate $E_T(t-\tau_D)$ and $E_p(t-\tau)$ by delta functions. In this case, Eq. (24) reduces to $S(\tau_D) \propto [\sum_j \kappa_j \kappa'_j / (M_j\omega_j) Z_j(\tau_D)]^2$, which recovers the previous result.^{1,2}

When the thermal motions of the bath are fast compared with the oscillator motion, the s dependence of $\gamma_j(s)$ is weak and can be neglected, i.e., $\gamma_j(s) = \gamma_j(s=0) \equiv \gamma_j$. In this case we can perform the inverse Laplace transform in Eq. (23) resulting in^{1,2}

onstrates the filtering effect of pulse shaping [cf. Eq. (15)] which allows only selected Fourier components of optical medium $R(\omega)$ to be observed and discriminates against other frequency components. It should be noted that the pulse train selects the Fourier component of nuclear motion, rather

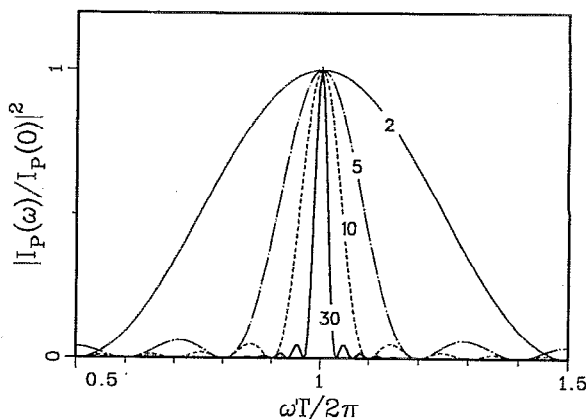


FIG. 1. The spectrum $|I_p(\omega)/I_p(0)|^2$ [Eq. (16a) or (27)] of the pump train of N identical ultrashort pulses [Eq. (26)] vs $\omega T/2\pi$. T is the pulse repetition time in the pump train and $I_p(\omega) = I_p(\omega + 2\pi/T)$ is a periodic function. The various curves correspond to different values of N as indicated. As the number of pulses N increases, $I_p(\omega)$ becomes more sharply peaked around $\omega = 2\pi n/T$, with $n = 1, 2, \dots$, and the frequency selectivity of the pump field is improved.

er than the microscopic molecular mode that may be subject to dissipation and random force from the solvent as well as anharmonicities. As the number of pulses N increases, the spectral width of the frequency filtering function narrows. In

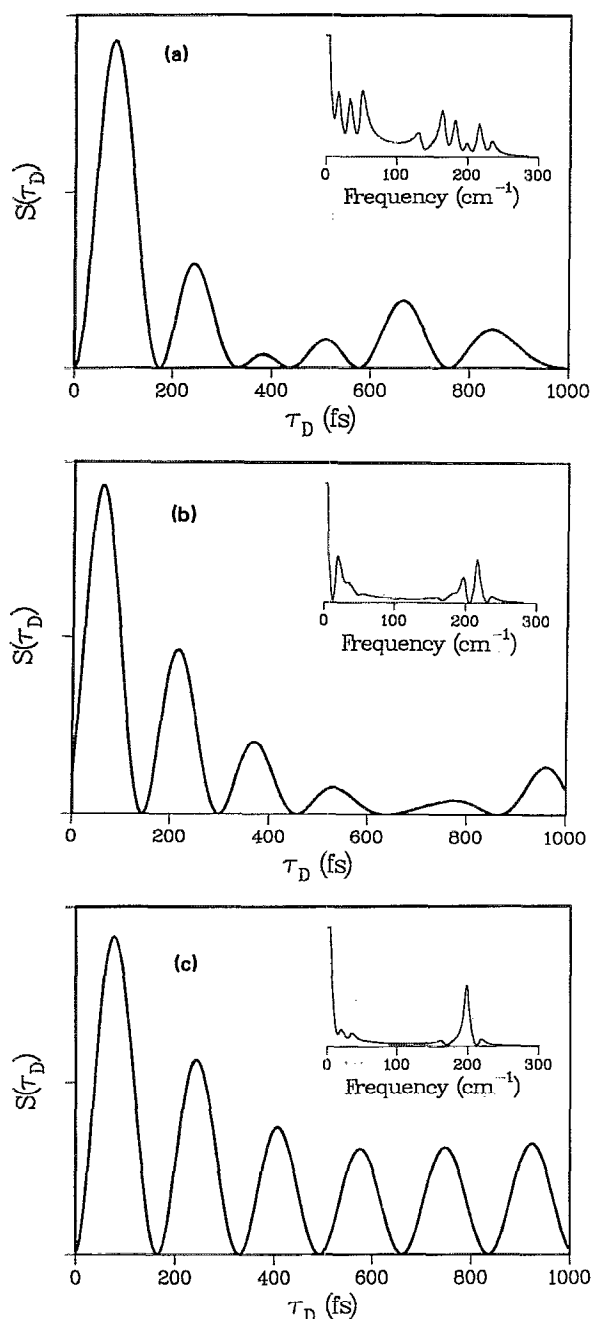


FIG. 2. (a) The Raman signal $S(\tau_D)$ [Eq. (24)] of a Brownian harmonic molecule [Eq. (25)] with three modes: $\omega_1 = 100 \text{ cm}^{-1}$, $\omega_2^* = 67 \text{ cm}^{-1}$, and $\omega_3 = 117 \text{ cm}^{-1}$, the friction parameters $\gamma_1 = \gamma_2 = \gamma_3 = 5 \text{ cm}^{-1}$ and coupling $\kappa_1 \kappa'_1 / (M_1 \omega_1) = \kappa_2 \kappa'_2 / (M_2 \omega_2) = \kappa_3 \kappa'_3 / (M_3 \omega_3)$. The calculation is performed in the impulsive limit where both the probe and the pump fields are a single peaked ($N = 1$) ultrashort pulses. The power spectrum of the Raman signal is shown in the insert. No mode selectivity is observed. (b) The same as (a) but for the shaped pump train of $N = 3$ pulses [Eq. (26)], and $T = 334 \text{ fs}$ (or $1/cT = 100 \text{ cm}^{-1}$). The optical selectivity for mode 1 ($\omega_1 = 100 \text{ cm}^{-1}$) is developed. (c) The same as (b) but for a longer pump train with $N = 30$. The optical selectivity for mode 1 ($\omega_1 = 100 \text{ cm}^{-1}$) is now clear.

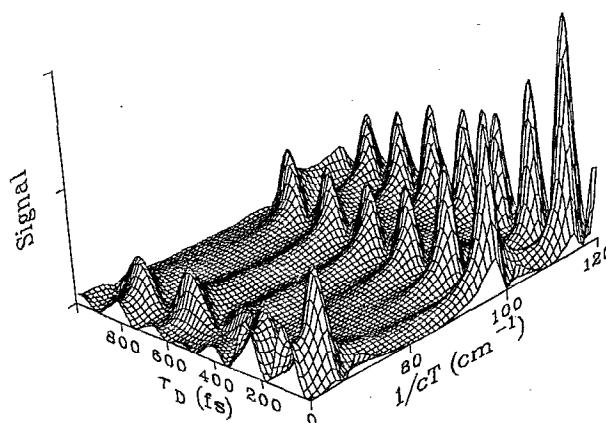


FIG. 3. The Raman signal $S(\tau_D)$ vs the delay time τ_D and the repetition time T for the same model molecule in Fig. 2(c). The pump field is given by Eq. (26) with $N = 30$. The three modes are well resolved at different values of T .

the ideal case where $N \rightarrow \infty$, the spectral profile of the pump field becomes a series of delta functions and the Raman excitation selects only the coherent Raman modes with $\omega_j = 2n\pi/T$, $n = 1, 2, \dots$ (assuming $\gamma_j = 0$). The selected mode motion is not amplified by splitting up a single pulse into many pulses with the same total amount of energy. We next present the Raman signal of a three mode system to demonstrate this filtering effect. Figure 2(a) is the impulsive (nonselective) limit ($N = 1$). Figure 2(b) and (c) shows the signals pumped by a train of 3 and 30 pulses, respectively, with repetition time $T = 334 \text{ fs}$ (corresponding to a vibrational frequency of 100 cm^{-1}). The frequency selectivity of pulse shaping is demonstrated. In Figure 3, we present the Raman signal for the same model system with $N = 30$ versus the time delay τ_D and the train period T . The 67, 100, and 117 cm^{-1} modes are clearly separated and show up at different values of the train period.

V. DISCUSSION

In the previous section we analyzed the filtering effect of Raman excitation using pulse shaping, which allows us to observe the motions of a few selected Raman modes. It was suggested that the off resonant Raman excitation can also be used as a means of laser controlled chemistry.⁶ Below, we analyze this possibility by examining the doorway state prepared by a properly shaped pump excitation of the j th driven Brownian harmonic oscillator [Eqs. (21)]. The doorway state can in this case be factorized as $\rho(t) = \prod_j \rho_j(t)$. In the Wigner (phase space) representation we have^{11,12}

$$\rho(\mathbf{p}, \mathbf{q}; t) = \prod_j \rho(p_j, q_j; t), \quad (28a)$$

with

$$\rho(p_j, q_j; t) = \frac{\omega_j}{2\pi\xi_j} \exp \left\{ -\frac{M_j \omega_j^2}{2\xi_j} [q_j - \langle q_j(t) \rangle]^2 - \frac{1}{2M_j \xi_j} [p_j - \langle p_j(t) \rangle]^2 \right\} \dots \quad (28b)$$

Alternatively, we may expand the doorway density matrix in the vibronic state representation:

$$\rho(v, v'; t) = \prod_j \langle v_j | \rho_j(t) | v'_j \rangle \equiv \prod_j \rho(v_j, v'_j; t), \quad (29a)$$

where

$$\begin{aligned} \rho(v_j, v'_j; t) &= (\bar{n}_j + 1)^{-(v_j + v'_j + 1)} (v_j! v'_j!)^{-1/2} \\ &\times \exp[-|A_j(t)|^2 / (\bar{n}_j + 1)] \\ &\times \sum_{l=0}^{l_M} \frac{v_j! v'_j!}{l! (v_j - l)! (v'_j - l)!} \\ &\times [\bar{n}_j (\bar{n}_j + 1)]^l [A_j(t)]^{v_j - l} [A_j^*(t)]^{v'_j - l}. \end{aligned} \quad (29b)$$

Here, the summation in Eq. (29b) runs up to $l_M = \min(v_j, v'_j)$. In Eq. (28b), $\langle q_j(t) \rangle$ and $\langle p_j(t) \rangle$ are the expectation values of the coordinate and momentum of the j th mode in the doorway state:

$$\begin{aligned} \langle q_j(t) \rangle &\equiv \text{Tr}[q_j \rho(t)] \\ &= -(M_j \omega_j)^{-1} \int_0^\infty d\tau F_j(t - \tau) Z_j(\tau), \end{aligned} \quad (30a)$$

$$\begin{aligned} \langle p_j(t) \rangle &\equiv \text{Tr}[p_j \rho(t)] \\ &= -\omega_j^{-1} \int_0^\infty d\tau F_j(t - \tau) \dot{Z}_j(\tau), \end{aligned} \quad (30b)$$

and in Eq. (29b),

$$\begin{aligned} A_j(t) &= (M_j \omega_j / 2\hbar)^{1/2} \langle q_j(t) \rangle \\ &\quad + i(2\hbar M_j \omega_j)^{-1/2} \langle p_j(t) \rangle. \end{aligned} \quad (31)$$

At zero temperature, $\bar{n}_j = 0$ [Eq. (22b)] and the doorway state [Eq. (29)] represents a coherent state.¹⁷ Furthermore, $\langle q_j(t) \rangle$ is directly related to the Raman signal [Eq. (10)] via the relation:

$$\text{Tr}[\alpha_T \rho(t)] = \sum \kappa_j \langle q_j(t) \rangle. \quad (32)$$

In Eqs. (30), $F_j(\tau)$ is the driving force [Eq. (18b)], which pumps an excess energy of $\Delta \xi_j(t) = \hbar \omega_j |A_j(t)|^2$ to the j th Raman mode. If this mode represents a coherent vibration with $\gamma_j = 0$, we have $Z_j(t) = \sin \omega_j t$ and Eq. (31) reduces to

$$\begin{aligned} A_j(t) &= -i(2\hbar M_j \omega_j)^{-1/2} \\ &\times \int_{-\infty}^t d\tau \exp[-i\omega_j(t - \tau)] F_j(\tau). \end{aligned} \quad (33)$$

After the pump field, $A_j(t > 0)$ is proportional to $I_p(\omega_j)$, the pump field spectrum at frequency ω_j [cf. Eqs. (16a) and (18b)]. In the presence of finite friction $\gamma_j \neq 0$, the amplitude of the vibrational motions [Eq. (30)] decreases, as shown in Fig. 4. For simplicity we shall consider the possibility of Raman excitation controlled chemistry in the optimal case of $\gamma_j = 0$. Using the pulse train [Eq. (26)] we have

$$A_j(t) = -i\eta_j \exp(-i\omega_j t) I_p(\omega_j) / I_p(0), \quad (34a)$$

with

$$\eta_j = (2\hbar M_j \omega_j)^{-1/2} \int_{-\infty}^\infty d\tau F_j(\tau). \quad (34b)$$

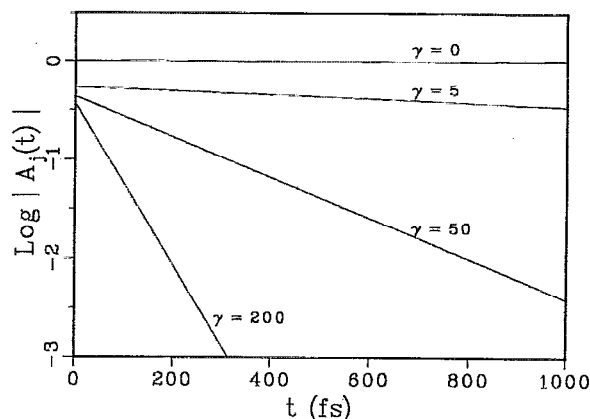


FIG. 4. The amplitude $|A_j(t)|$ [Eq. (31)] of $\omega_j = 100 \text{ cm}^{-1}$ oscillation motion for various values of friction γ_j (in cm^{-1}). The pump pulse train is the same as in Fig. 2(c) ($N = 30$, $T = 334 \text{ fs}$).

The amplitude of the coherent oscillation [Eq. (34a)] $|A_j(t)|$ is given by the product of η_j [Eq. (34b)] and $|I_p(\omega_j)/I_p(0)|$, the amplitude of the pump profile at ω_j [cf. Eq. (27)]. Consider an ordinary impulsive Raman experiment using a single pulse [Eq. (26) with $N = 1$]. In that case the amplitude in the coherent oscillation is given by $|A_j(t)| = \eta_j$ with all the Raman modes being equally excited. Consider now a Raman experiment conducted using a shaped train of ultrashort pulses with a fixed total energy [Eq. (26)]. If the repetition rate in the pulse train is tuned to match a particular Raman mode j , the pump profile $|I_p(\omega_j)/I_p(0)|$, which acts as a frequency filter function, excites only the j th, Raman mode, whose amplitude is unchanged by the pulse shaping, but discriminates against the other modes: $|A_k(t)| \approx 0$; $k \neq j$ (cf. Fig. 1).

Finally, we should comment on the implications of these results on laser selective chemistry. Tannor, Kosloff, and Rice,¹⁸ and Rabitz¹⁹ have studied the resonant laser control of reaction selectivity. The selectivity is controlled in that case by the excited state dynamics and the Franck-Condon overlaps between the ground and the excited electronic surfaces. It has been suggested⁶ that the Raman filtering may allow the selective pumping of molecular vibrations to high degrees of excitation, thereby promoting mode specific chemistry using off resonant pumping. By increasing the intensity of the pump field we increase the amplitude $|A_j(t)| = \eta_j$ of the selected j th oscillator. This amplitude is proportional to the intensity of the excitation field [cf. Eqs. (34b) and (18b)]. At low temperatures an impulsive light excitation prepares a coherent state⁶ whereby all the molecules are equally excited. A stronger Raman amplitude thus implies that each molecule undergoes a larger amplitude motion. This argument holds for classical as well as quantum oscillators since the doorway state in the Wigner representation [Eq. (28)] is identical for both cases. The picture is, however, very different if we examine the oscillator energy. In an ensemble of classical oscillators we find that all j type oscillators acquire the same excess energy $\Delta \xi_j(t)$. If we

measure the energy of quantum driven oscillators, we find that $\Delta\xi_j(t)$ represents only the *mean energy* acquired by the j oscillators but that the oscillator energy has a probability distribution. When the oscillator energy is measured, we find that the probability of the oscillator to be in its ν_j state is $\rho(\nu_j, \nu_j, t)$. By setting $\nu_j = \nu_j'$ and rearranging Eq. (29b) we have

$$\begin{aligned} \rho(\nu_j, \nu_j, t) = & \exp[-|A_j(t)|^2/(\bar{n}_j + 1)] \\ & \times \sum_{l=0}^{\nu_j} \frac{\nu_j!}{(\nu_j - l)!(l!)^2} \\ & \times (\bar{n}_j + 1)^{-2l} |A_j(t)|^{2l} \rho_{eq}(\nu_j - l, \nu_j - l). \end{aligned} \quad (35)$$

Here, $\rho_{eq}(\nu_j', \nu_j')$ is the initial thermal equilibrium population in the vibronic level $|\nu_j'\rangle$. Equation (35) shows that the contribution to the population of $|\nu_j\rangle$ resulting from the initial vibronic state $|\nu_j - l\rangle$ is of the order of $|A_j(t)|^{2l}$. We have shown that the upper bound of $|A_j(t)|^2$ is η_j^2 [cf. Eq. (34a)], which is obtained by exciting the selected coherent vibrational mode with $\gamma_j = 0$. As shown in Eqs. (34b) and (18b), η_j^2 depends on the non-Condon coefficient of the molecule κ_j , the Condon transition dipole μ_0 , the pump detuning parameter $\bar{\Omega}_p$, and is proportional to the square of the field intensity. Let us consider the typical value of η_j^2 in pulsed Raman scattering experiments of organic molecules,⁶ in which we assume the optical medium with $\kappa_j/(M_j\omega_j)^{1/2} = 0.1$ and $\mu_0 = 1$ D, subjected to a 5 μ J laser pulse with beam diameter of 0.1 mm and $\bar{\Omega}_p = 5000$ cm⁻¹. We have, in this case, $|A_j(t)|^2 < \eta_j^2 \approx 10^{-4}$, which using Eqs. (30a) and (31) corresponds to an increase in the macroscopic vibrational amplitude of ~ 0.01 Å for an oscillator with $\omega_j = 100$ cm⁻¹ and a proton mass. For such small value of η_j^2 , the molecule initially at $|\nu_j\rangle$ state can only be excited to $|\nu_j + 1\rangle$ state, as shown by Eq. (35). The probability of exciting to higher states is of the order of η_j^4 or higher and can be neglected. Therefore, as long as $\eta_j^2 \ll 1$, raising the energy of the pump field results in exciting more molecules from $|\nu_j\rangle$ to $|\nu_j + 1\rangle$ thereby increasing the macroscopic Raman polarization. The spectral filtering under typical conditions for the Raman experiment is therefore a *macroscopic* effect and does not involve exciting individual molecules to a high level of excitation, which is the primary requirement for mode specific chemistry. This is to be contrasted with electronically resonant excitation.¹⁸⁻²⁰

In summary, we presented an effective Hamiltonian [Eq. (5a)] which controls the molecular evolution under off resonant light excitation. This effective Hamiltonian applies for an arbitrary intensity and shape of the excitation field. In the off resonant regime, the optical response of a medium is characterized by its electronic polarizability [Eq. (5b)], which depends on the nuclear motions of the optically active modes. The resulting transient coherent Raman signal, to lowest order, depends on the response function of the polarizability [Eqs. (10) and (11)]. This result is also valid for a stationary coherent Raman¹³ and for pump-probe absorption spectroscopy.⁷ By assuming a weak (linear) dependence of the polarizability on the optically active mode, we recovered the driven oscillator model with the driving force

proportional to the intensity of the excitation field [Eq. (18)]. Finally, in Sec. IV, we presented a detailed model analysis of the effect of pulse shaping on optical and chemical selectivity of molecular systems. Since the shaped pulse train serves as a frequency filter, it does not amplify the molecular motion compared with excitation with a single pulse with the same total energy. Of course, amplification is possible if the pulse train has more total energy than a single pulse. In some materials, optical damage thresholds that limit the peak intensity of a single pulse may be circumvented by use of a pulse train, so that higher total energies can be used. The multiple pulse Raman experiments represent an interesting attempt to achieve a high degree of selectivity, whose chances should be viewed cautiously. Tailored pulse trains with variable train intervals may be required in order to pump anharmonic modes. Off resonance excitation typically pumps very small amount of energy and when the energy is measured its distribution shows a large number of weakly excited molecules rather than a small number of highly excited molecules (as is required for laser induced chemistry). High degree of selective excitation can however be easily achieved using resonant pumping.

ACKNOWLEDGMENTS

The support of the National Science Foundation, the Air Force Office of Scientific Research, and the Petroleum Research Fund, administered by the American Chemical Society, is gratefully acknowledged. We wish to thank W. Bosma for his assistance in the preparation of this article.

APPENDIX A: THE DOORWAY STATE AND THE EFFECTIVE HAMILTONIAN H_{eff} : DERIVATION OF EQS. (4)

The density matrix of our system with a classical pump field satisfies the Liouville equation:

$$\begin{aligned} \dot{\rho}_T(\mathbf{r}, t) = & -(i/\hbar) [H, \rho_T(\mathbf{r}, t)] \\ & + (i/\hbar) E_P(\mathbf{r}, t) [V, \rho_T(\mathbf{r}, t)]. \end{aligned} \quad (\text{A1})$$

Here, H is the total Hamiltonian of the material system [Eq. (1b)]; E_P is the electric field of the pump pulse [Eq. (2b)]. As shown in Eq. (3), we shall expand $\rho_T(\mathbf{r}, t)$ as a 2×2 matrix in the electronic space and keep each matrix element as an operator in the nuclear space. The Liouville equation [Eq. (A1)] thus reads:

$$\begin{aligned} \dot{\rho}_{gg}(\mathbf{r}, t) = & -i\mathcal{L}_{gg}\rho_{gg}(\mathbf{r}, t) + iE_P(\mathbf{r}, t) \\ & \times [\mathcal{V}_{gg, eg}\rho_{eg}(\mathbf{r}, t) + \mathcal{V}_{gg, ge}\rho_{ge}(\mathbf{r}, t)], \end{aligned} \quad (\text{A2a})$$

$$\begin{aligned} \dot{\rho}_{ee}(\mathbf{r}, t) = & -i\mathcal{L}_{ee}\rho_{ee}(\mathbf{r}, t) + iE_P(\mathbf{r}, t) \\ & \times [\mathcal{V}_{ee, ge}\rho_{ge}(\mathbf{r}, t) + \mathcal{V}_{ee, eg}\rho_{eg}(\mathbf{r}, t)], \end{aligned} \quad (\text{A2b})$$

$$\begin{aligned} \dot{\rho}_{eg}(\mathbf{r}, t) = & -i(\mathcal{L}_{eg} + \omega_{eg})\rho_{eg}(\mathbf{r}, t) + iE_P(\mathbf{r}, t) \\ & \times [\mathcal{V}_{eg, gg}\rho_{gg}(\mathbf{r}, t) + \mathcal{V}_{eg, ee}\rho_{ee}(\mathbf{r}, t)], \end{aligned} \quad (\text{A2c})$$

$$\begin{aligned} \dot{\rho}_{ge}(\mathbf{r}, t) = & -i(\mathcal{L}_{ge} - \omega_{eg})\rho_{ge}(\mathbf{r}, t) + iE_P(\mathbf{r}, t) \\ & \times [\mathcal{V}_{ge, ee}\rho_{ee}(\mathbf{r}, t) + \mathcal{V}_{ge, gg}\rho_{gg}(\mathbf{r}, t)], \end{aligned} \quad (\text{A2d})$$

where \mathcal{L}_{mn} and $\mathcal{V}_{mn, m'n'}$, with $m, n, m', n' = g, e$, are the Liouville space operators defined by their actions to an arbitrary dynamical variable A :

$$\mathcal{V}_{mn,m'n'}A \equiv \hbar^{-1} [\delta_{nn'}(1 - \delta_{mm'})\mu A - A\mu(1 - \delta_{nn'})\delta_{mm'}], \quad (\text{A3a})$$

$$\mathcal{L}_{mn}A \equiv \hbar^{-1} [H_m A - A H_n]. \quad (\text{A3b})$$

We further define the Green's function $\mathcal{G}_{mn}(t)$ associating with \mathcal{L}_{mn} by

$$\mathcal{G}_{mn}(t)A = \exp(-iH_m t/\hbar)A \exp(iH_n t/\hbar); \quad m, n = e, \text{ or } g. \quad (\text{A4})$$

In the absence of nuclear degrees of freedom, $\mathcal{L}_{mn} = 0$, $\mathcal{G}_{mn}(t) = 1$, $\mathcal{V}_{mn,m'n'} = \mu_{eg}/\hbar$, and Eqs. (A2) reduces to the optical Bloch equations.

The formal solution to the generalized Bloch equations (A2) can be obtained as follows: The electronic coherences ρ_{mn} with $m \neq n$ can be expressed in terms of the electronic populations ρ_{gg} and ρ_{ee} by a direct integration of Eqs. (A2c) and (A2d), with the initial conditions $\rho_{eg}(-\infty) = \rho_{ge}(-\infty) = 0$. We then have,

$$\rho_{eg}(\mathbf{r}, t) = i \int_{-\infty}^t d\tau E_P(\mathbf{r}, \tau) \exp[-i\omega_{eg}(t - \tau)] \times \mathcal{G}_{eg}(t - \tau) [\mathcal{V}_{eg,gg}\rho_{gg}(\mathbf{r}, \tau) + \mathcal{V}_{eg,ee}\rho_{ee}(\mathbf{r}, \tau)]. \quad (\text{A5})$$

Its Hermitian conjugate $\rho_{ge} = [\rho_{eg}]^\dagger$ can be obtained from Eq. (A5) by simply interchanging the indexes g and e . Closed equations of motion for the electronic populations can then be obtained by substituting ρ_{eg} [Eq. (A5)] and its Hermitian conjugate ρ_{ge} for (A2a) and (A2b). We thus have,

$$\begin{aligned} \dot{\rho}_{gg}(\mathbf{r}, t) = & -i\mathcal{L}_{gg}\rho_{gg}(\mathbf{r}, t) \\ & - \int_{-\infty}^t d\tau \mathcal{K}(t; \tau) \rho_{gg}(\mathbf{r}, \tau) \\ & + \int_{-\infty}^t d\tau \mathcal{K}'(t; \tau) \rho_{ee}(\mathbf{r}, \tau), \end{aligned} \quad (\text{A6})$$

with

$$\begin{aligned} \mathcal{K}(t; \tau) = & E_P(\mathbf{r}, t)E_P(\mathbf{r}, \tau) \exp[-i\omega_{eg}(t - \tau)] \\ & \times \mathcal{V}_{gg,eg}\mathcal{G}_{eg}(t - \tau)\mathcal{V}_{eg,gg} \\ & + E_P(\mathbf{r}, t)E_P(\mathbf{r}, \tau) \exp[i\omega_{eg}(t - \tau)] \\ & \times \mathcal{V}_{gg,ge}\mathcal{G}_{ge}(t - \tau)\mathcal{V}_{ge,gg}, \end{aligned} \quad (\text{A7a})$$

$$\begin{aligned} \mathcal{K}'(t; \tau) = & -E_P(\mathbf{r}, t)E_P(\mathbf{r}, \tau) \exp[-i\omega_{eg}(t - \tau)] \\ & \times \mathcal{V}_{gg,eg}\mathcal{G}_{eg}(t - \tau)\mathcal{V}_{eg,ee} \\ & - E_P(\mathbf{r}, t)E_P(\mathbf{r}, \tau) \exp[i\omega_{eg}(t - \tau)] \\ & \times \mathcal{V}_{gg,ge}\mathcal{G}_{ge}(t - \tau)\mathcal{V}_{ge,ee}. \end{aligned} \quad (\text{A7b})$$

Here, $\rho_{ee}(\mathbf{r}, t)$ satisfies a similar equation of motion that can be obtained from Eqs. (A6) and (A7) by simply interchanging the indexes g and e . The first term in rhs of Eq. (A6) describes the adiabatic motions of the system in the electronic ground state in the absence of the external field. Also, $\mathcal{K}(t - \tau)$ [Eq. (A7a)] is a Liouville space operator representing the nuclear relaxation processes, following the electronic excitation, within the g state as well as the loss of population from g to e ; $\mathcal{K}'(t - \tau)$ [Eq. (A7b)] represents processes in which the system transfers from e to g . Equations of motion for $\rho_{gg}(\mathbf{r}, t)$ [Eq. (A6)] and $\rho_{ee}(\mathbf{r}, t)$ constitute the generalized master equations for the optical system. If we specify the representation, Eq. (A6) can be recast more explicitly as

$$\begin{aligned} \dot{\rho}_{gg}(\Gamma, t) = & -i \int d\Gamma' \mathcal{L}_{gg}(\Gamma; \Gamma') \rho_{gg}(\Gamma', t) \\ & - \int_{-\infty}^t d\tau \int d\Gamma' \mathcal{K}(\Gamma, t; \Gamma', \tau) \rho_{gg}(\Gamma', \tau) \\ & + \int_{-\infty}^t d\tau \int d\Gamma' \mathcal{K}'(\Gamma, t; \Gamma', \tau) \rho_{ee}(\Gamma', \tau). \end{aligned} \quad (\text{A8a})$$

Here, Γ stands for the molecular nuclear degrees of freedom and it depends on the choice of representation. In the Wigner representation, $\Gamma = \mathbf{pq}$ and

$$\int d\Gamma' = \iint d\mathbf{p}' d\mathbf{q}' \quad (\text{A8b})$$

represents the integration over the entire phase space of the nuclear degrees of freedom. However, in the vibronic eigenstate representation, $\Gamma = \mathbf{vv}'$ and

$$\int d\Gamma' = \sum_{\mathbf{v}\mathbf{v}'} \quad (\text{A8c})$$

Consider the kernel \mathcal{K} or \mathcal{K}' [Eqs. (A7)]. The spatial direction and the optical phase factors associating with the kernel are determined by the product of the pump fields. From Eq. (2b), we have

$$\begin{aligned} E_P(\mathbf{r}, t)E_P(\mathbf{r}, \tau) = & 2[1 + \cos(\mathbf{k}_1 - \mathbf{k}_2) \cdot \mathbf{r}] E_P^*(t)E_P(\tau) \exp[i\Omega_P(t - \tau)] \\ & + [\exp(i\mathbf{k}_1 \cdot \mathbf{r}) + \exp(i\mathbf{k}_2 \cdot \mathbf{r})]^2 E_P(t)E_P(\tau) \exp(-i2\Omega_P t) \exp[i\Omega_P(t - \tau)] + c.c. \end{aligned} \quad (\text{A9})$$

The key quantity in the calculation of the kernel $\mathcal{K}(\Gamma, t; \Gamma', \tau)$ or $\mathcal{K}'(\Gamma, t; \Gamma', \tau)$ [Eqs. (A7)] is the generalized Green's function $\mathcal{G}_{mn}(\Gamma, t - \tau; \Gamma')$ [Eq. (A4)], whose evolution is governed from the left and from the right by different adiabatic Hamiltonians. The equation of motion for \mathcal{G}_{mn} , which is exact for the harmonic system or for the short time propagation of the anharmonic system, has been

developed recently.¹¹

Consider an off resonant excitation optical processes in which $|\Omega_P \pm \omega_{eg}|$ are large compared with the inverse timescales of the pulse duration, and the nuclear dynamics. In this case, the optical phase contributions to the integrand in the rhs of Eq. (A6) are fast varying quantities and we can consider the slowly varying amplitude of the integrand only

at $\tau = t$. We thus can make use of

$$E_P^*(t)E_P(\tau) \approx |E_P(t)|^2 \quad (\text{A10a})$$

and

$$\rho_{mm}(\mathbf{r}, \tau) \approx \rho_{mm}(\mathbf{r}, t), \quad m = e \text{ or } g, \quad (\text{A10b})$$

in evaluating the last two terms of Eq. (A6). Furthermore, for off resonant optical processes, we may neglect also the molecular nuclear dynamics in the optical coherence Green's function $\mathcal{G}_{eg}(t - \tau)$ or $\mathcal{G}_{ge}(t - \tau)$ and consider only the asymptotic behavior of the electronic dephasing processes by assuming ($m \neq n$):

$$-i \int_0^\infty d\tau \exp[i(\Omega_P \pm \omega_{eg})\tau] \mathcal{G}_{mn}(\tau) = \frac{1}{\Omega_P \pm \omega_{eg} - \Delta(\Omega_P \pm \omega_{eg}) + i\gamma(\Omega_P \pm \omega_{eg})}. \quad (\text{A10c})$$

Here, $\Delta(\omega) = -\Delta(-\omega)$ and $\gamma(\omega) = \gamma(-\omega)$ represents a frequency-dependent level shift and dephasing rate, respectively. For extreme off resonant detunings we have $|\Omega_P \pm \omega_{eg}| \gg \Delta(\Omega_P \pm \omega_{eg})$ and $\gamma(\Omega_P \pm \omega_{eg})$. Finally, the second term in Eq. (A9) and its complex conjugate make a negligibly small contribution when we make an optical cycle average and integrate Eq. (A6) in the off resonant configuration, since they contain the optical phase factor $\exp(\pm i2\Omega_P t)$. Making use of Eqs. (A10), we find in Eq. (A9) that term with the kernel \mathcal{K}' is negligibly small with the order of

$$[\rho_{eg}(\mathbf{r}, t) + \rho_{ge}(\mathbf{r}, t)]_{\mathbf{k}_S} = i \exp(i\mathbf{k}_S \mathbf{r} - i\Omega_T t) \int_{-\infty}^t d\tau E_T(\tau - \tau_D) \times \{ \exp[i(\Omega_T - \omega_{eg})(t - \tau)] \mathcal{G}_{eg}(t - \tau) \mathcal{V}_{eg,gg} + \exp[i(\Omega_T + \omega_{eg})(t - \tau)] \mathcal{G}_{ge}(t - \tau) \mathcal{V}_{ge,gg} \} \rho_{gg}(\mathbf{r}, \tau). \quad (\text{B2})$$

In the off resonant probe configuration, where $|\Omega_T \pm \omega_{eg}|$ is large compared with the inverse time scales of probe pulse and molecular dynamics, Eq. (B2) assumes the form:

$$[\rho_{eg}(\mathbf{r}, t) + \rho_{ge}(\mathbf{r}, t)]_{\mathbf{k}_S} = \exp(i\mathbf{k}_S \mathbf{r} - i\Omega_T t) E_T(t - \tau_D) \times \left[\frac{-\mu \rho_{gg}(\mathbf{r}, t)}{\Omega_T - \omega_{eg} - \Delta(\Omega_T - \omega_{eg}) + i\gamma(\Omega_T - \omega_{eg})} + \frac{\rho_{gg}(\mathbf{r}, t) \mu}{\Omega_T + \omega_{eg} - \Delta(\Omega_T + \omega_{eg}) + i\gamma(\Omega_T + \omega_{eg})} \right], \quad (\text{B3})$$

where we have made use of Eq. (A10c). Equation (9) can now be obtained by substituting Eqs. (B1) and (B3) in Eq. (8).

¹ Y. X. Yan, L. T. Cheng, and K. A. Nelson, *Advances in Nonlinear Spectroscopy*, edited by R. J. H. Clark and R. E. Hester (Wiley, New York, 1988), p. 299.

² K. A. Nelson and E. P. Ippen, *Adv. Chem. Phys.* **75**, 1 (1989).

³ (a) J. Chesnoy and A. Mokhtari, *Phys. Rev. A* **38**, 3566 (1988); (b) I. A. Walmsley, F. W. Wise, and C. L. Tang, *Chem. Phys. Lett.* **154**, 315 (1989); (c) A. M. Walsh and R. F. Loring, *Chem. Phys. Lett.* **160**, 299 (1989).

⁴ C. Kalpouzos, D. McMorro, W. T. Lotshaw, and G. A. Kenney-

$\gamma(\Omega_P \pm \omega_{eg})/(\Omega_P \pm \omega_{eg})^2$, whereas the term with the kernel \mathcal{K} has two contributions; one is real, which is also negligibly small with the same magnitude of \mathcal{K}' , and the other is pure imaginary which is proportional to $1/(\Omega_P \pm \omega_{eg})$. The later is the only surviving contribution to the off resonant excitation processes. Equation (A6) thus reduces to Eqs. (4) and (5). Equations of motion for $\rho_{ee}(t)$ in the far-off-resonance limit can be obtained in a similar way. Since in the present model $\rho_{ee}(\mathbf{r}, -\infty) = 0$, we find that $\rho_{ee}(\mathbf{r}, t) \approx 0$ and no excited state population is created.

APPENDIX B: THE PROBE SCATTERING: DERIVATION OF EQ. (9)

In this appendix, we present the optical polarization for a weak probe field following the off resonant pump process. Let us consider the optical polarization at time t :

$$P(\mathbf{r}, t) = \text{Tr}\{V\rho_T(\mathbf{r}, t)\} = \text{Tr}\{\mu[\rho_{eg}(\mathbf{r}, t) + \rho_{ge}(\mathbf{r}, t)]\}. \quad (\text{B1})$$

Here we have made use of Eqs. (1c) and (3). By assuming the separation of the pump and the probe fields, the optical coherence $\rho_{eg}(\mathbf{r}, \tau)$ with weak probe is similar to Eq. (A5), with replacing the pump field E_P by the probe E_T , and $\rho_{gg}(\mathbf{r}, \tau)$ and $\rho_{ee}(\mathbf{r}, \tau)$ being the doorway state prepared by pump field. As shown in Appendix A, in the off resonant pump configuration $\rho_{ee}(\mathbf{r}, \tau) \approx 0$ and $\rho_{gg}(\mathbf{r}, \tau)$ is given by Eqs. (4) and (5). The relevant optical coherence related to the polarization at $\mathbf{k}_S = \mathbf{k}_3 + \mathbf{k}_1 - \mathbf{k}_2$ is therefore given by

Wallace, *Chem. Phys. Lett.* **150**, 138 (1988); D. McMorro, W. T. Lotshaw, *Chem. Phys. Lett.* **174**, 85 (1990).

⁵ A. M. Weiner, J. P. Heritage, and E. M. Kirschner, *J. Opt. Soc. Am. B* **5**, 1563 (1988); A. M. Weiner, J. P. Heritage, and J. A. Salehi, *Opt. Lett.* **13**, 300 (1988); A. M. Weiner and D. E. Leaird, *Opt. Lett.* **15**, 51 (1990); A. M. Weiner, D. E. Leaird, J. S. Patel and J. R. Wullert, *Opt. Lett.* **15**, 326 (1990).

⁶ A. M. Weiner, D. E. Leaird, G. P. Wiederrecht, and K. A. Nelson, *Science* **247**, 1317 (1990).

⁷ Y. J. Yan and S. Mukamel, submitted to *Phys. Rev. A*; Y. J. Yan, L. E. Fried, and S. Mukamel, *J. Phys. Chem.* **93**, 8149 (1989).

⁸ R. W. Hellwarth, *Prog. Quant. Elec.* **5**, 1 (1977).

⁹ S. Mukamel, *Adv. Chem. Phys.* **70**, Part I, 165 (1988).

¹⁰ S. Mukamel and R. F. Loring, *J. Opt. Soc. Am. B* **3**, 595 (1986).

¹¹ Y. J. Yan and S. Mukamel, *J. Chem. Phys.* **89**, 5160 (1988).

¹² Y. J. Yan and S. Mukamel, *J. Chem. Phys.* **86**, 6085 (1988).

¹³ S. Mukamel, *Ann. Rev. Phys. Chem.* **41**, 647 (1990).

¹⁴ J. Tang and A. C. Albrecht, in *Raman Spectroscopy*, edited by H. A. Szymanski (Plenum, New York, 1970), Vol. 2, p. 33.

¹⁵ D. Forster, *Hydrodynamic Fluctuations, Broken Symmetry, and Correlation Functions* (Benjamin, New York, 1975).

¹⁶ S. A. Adelman, *J. Chem. Phys.* **64**, 124 (1976).

¹⁷ W. H. Louisell, *Quantum Statistical Properties of Radiation* (Wiley, New York, 1973).

¹⁸ R. Kosloff, S. A. Rice, P. Gaspard, S. Tersigni, and D. J. Tannor, *Chem. Phys.* **139**, 201 (1989); D. J. Tannor, R. Kosloff, and S. A. Rice, *J. Chem. Phys.* **85**, 5805 (1986).

¹⁹ S. Shi, A. Woody, and H. Rabitz, *J. Chem. Phys.* **88**, 6870 (1988).

²⁰ A. H. Zewail, *Science* **242**, 1645 (1988).